Clinical Neurophysiology 157 (2024) 146–155

Contents lists available at ScienceDirect

Clinical Neurophysiology

journal homepage: www.elsevier.com/locate/clinph

Parkinsonian rest tremor can be distinguished from voluntary hand movements based on subthalamic and cortical activity

Dmitrii Todorov [a,b,c], Alfons Schnitzler [a,d], Jan Hirschmann [a,*]

[a] Institute of Clinical Neuroscience and Medical Psychology, Medical Faculty and University Hospital Düsseldorf, Heinrich Heine University Düsseldorf, Germany
[b] Centre de Recherche en Neurosciences de Lyon - Inserm U1028, 69675 Bron, France
[c] Centre de Recerca Matemática, Campus UAB edifici C, 08193 Bellaterra, Barcelona, Spain
[d] Center for Movement Disorders and Neuromodulation, Department of Neurology Medical Faculty, Heinrich Heine University, 40225 Düsseldorf, Germany

See Editorial, pages 143–145

HIGHLIGHTS

- Brain activity allows for distinguishing Parkinsonian tremor from voluntary movements.
- Subthalamic nucleus activity alone is not sufficient for the distinction; cortical data is required for this.
- Dopaminergic medication does not affect classification performance.

ARTICLE INFO

Article history:
Accepted 31 October 2023
Available online 17 November 2023

Keywords:
Tremor
Voluntary movements
Parkinson's disease
MEG
Subthalamic nucleus
Classification
Machine learning

ABSTRACT

Objective: To distinguish Parkinsonian rest tremor and different voluntary hand movements by analyzing brain activity.
Methods: We re-analyzed magnetoencephalography and local field potential recordings from the subthalamic nucleus of six patients with Parkinson's disease. Data were obtained after withdrawal from dopaminergic medication (Med Off) and after administration of levodopa (Med On). Using gradient-boosted tree learning, we classified epochs as tremor, fist-clenching, forearm extension or tremor-free rest.
Results: Subthalamic activity alone was insufficient for distinguishing the four different motor states (balanced accuracy mean: 38%, std: 7%). The combination of cortical and subthalamic features, in contrast, allowed for a much more accurate classification (balanced accuracy mean: 75%, std: 17%). Adding a single cortical area improved balanced accuracy by 17% on average, as compared to classification based on subthalamic activity alone. In most patients, the most informative cortical areas were sensorimotor cortical regions. Decoding performance was similar in Med On and Med Off.
Conclusions: Electrophysiological recordings allow for distinguishing several motor states, provided that cortical signals are monitored in addition to subthalamic activity.
Significance: By combining cortical recordings, subcortical recordings and machine learning, adaptive deep brain stimulation systems might be able to detect tremor specifically and to respond adequately to several motor states.

1. Introduction

Deep brain stimulation (DBS) is a widely used treatment for advanced Parkinson's disease (PD) (Krauss et al., 2021). While well accepted and effective, it also has significant side-effects (Zarzycki and Domitrz, 2020) most of which result from current spread to structures adjacent to the DBS target (Koeglsperger et al., 2019). Hence, a general strategy for reducing side-effects is to reduce the energy applied in DBS. One way to achieve this while maintaining clinical benefits is to adapt stimulation to the current motor state. This approach is called adaptive DBS (Krauss et al., 2021; Meidahl et al., 2017; Neumann et al., 2019). Various signals can be used to control either the onset or the amplitude of DBS

* Corresponding author at: Institute of Clinical Neuroscience and Medical Psychology, Medical Faculty, Heinrich Heine University, Moorenstraße 5, 40225 Düsseldorf, Germany.
E-mail address: jan.hirschmann@med.uni-duesseldorf.de (J. Hirschmann).

https://doi.org/10.1016/j.clinph.2023.10.018
1388-2457/

(Marceglia et al., 2021). Currently, the most investigated neural control signal is subthalamic beta band activity (Little et al., 2016, 2013; Piña-Fuentes et al., 2017; Tinkhauser et al., 2017), but other signals have also been considered, such as cortical gamma band activity (Gilron et al., 2021; Swann et al., 2018) or local evoked potentials (Dale et al., 2022).

Adapting DBS to the current motor state makes sense for treating tremor, particularly, because tremor is highly variable, waxing and waning spontaneously. In case of tremor, one natural strategy for adaptive DBS is to monitor tremor directly by means of peripherals such as accelerometers or electromyography (Cagnan et al., 2017; Cernera et al., 2021; Malekmohammadi et al., 2016). This approach, however, requires additional hardware and thus raises additional security and compliance issues.

An alternative strategy is to use brain signals rather than peripherals. It is known that Parkinsonian rest tremor originates in the brain (Milosevic et al., 2018), involving an extended subcortico-cortical network including the basal ganglia, cerebellum, thalamus and motor cortex (Helmich, 2018; Timmermann et al., 2003). Thus, it should be feasible to track tremor by monitoring its neural correlates. Several studies have investigated subcortical correlates by analyzing local field potentials (LFPs) recorded from DBS electrodes and identified numerous tremor-related changes, such as an increase of power at individual tremor frequency (Hirschmann et al., 2013a), a beta power decrease (Qasim et al., 2016; Wang et al., 2005), an increase of low gamma power (Beudel et al., 2015), and a shift of power in the very high frequency range (Hirschmann et al., 2016). While these studies were able to distinguish tremor from tremor-free rest periods, no study has been able to distinguish PD rest tremor from voluntary hand movements so far. When applying adaptive DBS in practice, it would be desirable to make this distinction to reduce unnecessary stimulation.

In this study, we re-analyzed simultaneous recordings of forearm EMG, magnetoencephalography (MEG) and subthalamic nucleus LFP data, obtained from tremor-dominant PD patients, aiming to distinguish between PD rest tremor, self-paced fist-clenching, static forearm extension and tremor-free rest periods (referred to as "quiet" episodes from here on), by means of gradient-boosted tree learning, a popular method in machine learning. We show that these motor states can be distinguished when considering cortical and subthalamic data.

2. Methods

2.1. Participants

In this study we used a subset of previously collected data (Hirschmann et al., 2013a). We selected patients with enough data for comparing rest tremor, quiet episodes, and two motor tasks (see below). Recordings from 6 patients met these requirements. We the kept participant identifiers consistent with (Hirschmann et al., 2013a). Overall, we had 11 datasets (5 subjects in Med On and Med Off, one subject in Med Off only; see Table 1).

All patients involved were diagnosed with idiopathic PD, and underwent DBS surgery the day before measurement. They experienced spontaneous waxing and waning of rest tremor during the recordings. Patient details are provided in Table 1. The study was approved by the ethics committee of the Medical Faculty of the Heinrich Heine University Düsseldorf (Study No. 3209). It was carried out in accordance with the Declaration of Helsinki and required written informed consent.

2.2. Recordings

Patients were recorded one day after subthalamic nucleus (STN) electrode implantation with leads still externalized. All but one patients were recorded in two sessions: one session OFF oral dopaminergic medication for at least 12 h and one session ON medication; one patient had only the OFF medication session recorded. Subcutaneous apomorphine administration was paused 1.5–2 h before measurements started. Each session contained four parts: rest, motor task 1, rest, motor task 2. Rest periods lasted 5 min. Motor task 1 was static forearm extension ("hold") and motor task 2 was self-paced fist-clenching ("grasp") at approximately 1 Hz (Hirschmann et al., 2013b). Movements were performed with the symptom-dominant body side in five 1-min blocks which were interleaved by 1 min pauses to avoid fatigue. During rest and between the blocks of voluntary movement tremor appeared and disappeared spontaneously.

Local field potentials from the STN, the magnetoencephalogram (MEG; Vectorview, MEGIN) and the surface electromyogram (EMG) of the extensor digitorum communis and flexor digitorum superficialis muscles of both upper limbs were recorded simultaneously. The sampling rate was 2000 Hz. DBS electrodes were connected to the amplifier of the MEG system by externalized, non-ferromagnetic leads. Electrode contacts were referenced to the left mastoid and rearranged to a bipolar montage offline by subtracting signals from neighboring contacts. EMG electrodes were referenced to surface electrodes at the muscle tendons. A hardware filter was applied with a pass-band of 0.1–660 Hz.

2.3. EMG labeling

The hand performing the voluntary movements showed intermittent rest tremor in all subjects. In order to label the data, EMG data was 10 Hz high-pass filtered, rectified and smoothed with a 100 ms box-filter. Quiet periods were identified semi-automatically. Epochs with both EMG channels (forearm flexor and extensor) deflecting less than their respective 40% quantiles (computed using the data from the entire recording) were labeled as candidate quiet periods automatically and then adapted manually. Tremor and voluntary movements were labeled manually. Epochs with uncertain labels, as well as postural and kinetic tremor were discarded. When possible, "safety offsets" were included to ensure that different behavioral states were separated by at least 1 s to mitigate the risk of confusing states (Fig. 1A). The amount of data available per motor state is provided in Table 2. Among the epochs with tremor, the proportion of bilateral tremor was 70% (std = 36%) in the medication OFF condition and 61% (std = 40%) in the medication ON condition.

2.4. Electrode localization

The placement of DBS electrodes was reconstructed with the Lead-DBS software package; (Horn and Kühn, 2015) from preoperative MR and postoperative CT images (Fig. 1B). This was not possible for two out of six patients due to noisy CT images.

2.5. Preprocessing

The MEG sensor data and LFP data were resampled to 256 Hz to increase computation speed. MEG artifacts were identified as time periods when sensor data deflected more than 2.5 times the signal's 95%-trimmed mean in multiple sensors. Spatiotemporal signal space separation (Taulu and Simola, 2006) with a 10 s time window was applied to the MEG data, using the MNE toolbox (Gramfort et al., 2014). LFP artifacts were identified as periods with strong broadband modulation of the signal.

Table 1
Patient data. In the "Electrode model" column, M: 4-contact, non-segmented electrode by Medtronic (model 3389), S: 4-contact, non-segmented electrode by St. Jude Medical.

subj	Sex	Age (y)	Disease duration (y)	Tremor frequency (Hz)	Electrode model	Medication states recorded
S01	m	65	8	4	M	ON, OFF
S02	m	69	6	3.5	M	ON, OFF
S03	m	68	11	3	M	OFF
S04	m	68	2	4	S	ON, OFF
S05	m	52	11	6	S	ON, OFF
S07	m	59	6	4.5	M	ON, OFF

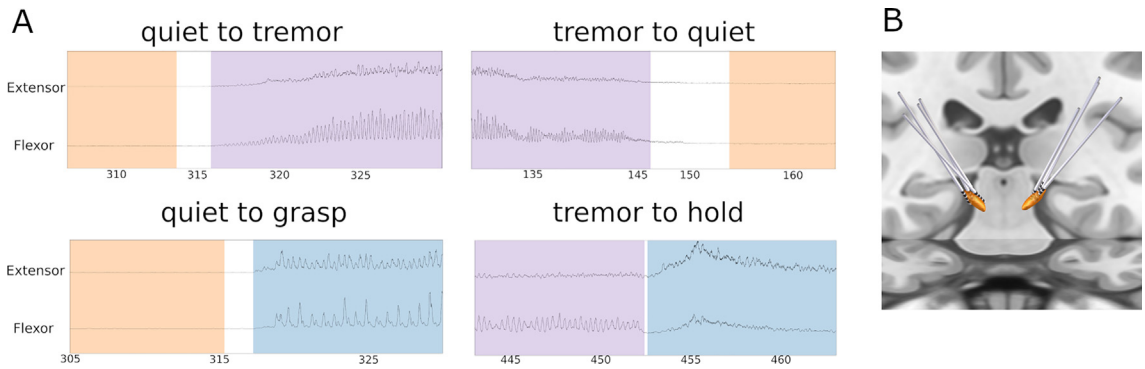

Fig. 1. Data labelling and electrode placement. A. Labeling of behavioral states in forearm EMG, state transition examples. B. Localization of deep brain stimulation (DBS) electrodes for four out of six patients. For two other patients (S02 and S03) the CT image quality was not sufficient for localization.

Table 2
Amount of data per motor state in seconds and balanced accuracy (bacc) in percent, for the feature set consisting of Hjorth activity of the best local field potential (LFP) channel and all cortical areas. The last column identifies the hand that was used to define the behavioral states. The amount refers to data used for classification, i.e. after discarding artifacts. N/A = not available.

subject	**tremor**	medication OFF			**bacc**	**tremor**	medication ON			**bacc**	**hand**
		quiet	**hold**	**grasp**			**quiet**	**hold**	**grasp**		
S01	240	384	307	238	91%	13	584	282	219	81%	left
S02	413	423	186	310	95%	350	169	311	320	79%	left
S03	16	434	335	253	45%	N/A	N/A	N/A	N/A	N/A	left
S04	56	403	252	119	73%	54	426	279	94	64%	left
S05	353	510	121	324	89%	18	539	293	261	87%	right
S07	77	451	258	236	47%	427	328	284	286	83%	left
mean	192.5	434.2	243.2	246.67	73%	172.4	409.2	289.8	236	78%	
std	167.19	43.92	78.74	72.828	22%	199.77	167.3	12.95	87.51	8%	

2.6. Source reconstruction

For forward modelling, we made use of realistic, single-shell head models based on the individual, T1-weighted MR image (Nolte, 2003). Source reconstruction was performed by means of Linearly Constrained Minimum Variance beamforming, as implemented in the Fieldtrip toolbox (Oostenveld et al., 2011). The beamformer grid contained 567 locations, spread out evenly across the cortical and cerebellar surface. It was aligned to Montreal Neurological Institute space, allowing for grid parcellation into 30 supersets of regions defined in the Automatic Anatomic Labeling atlas (Tzourio-Mazoyer et al., 2002). For the computation of the spatial filter, we used only the quiet periods without artifacts. For beamformer regularization, the lambda parameter was set to 0.1% of the maximum eigenvalue of the covariance matrix computed on the quiet periods.

2.7. Feature engineering

For feature engineering, the data were separated into 1 s-long disjoint windows, i.e. the temporal resolution was 1 s. Windows containing MEG or LFP artifacts were discarded. The number of windows per dataset averaged across subjects and medication conditions after artifact and uncertain EMG state rejection was 1112 (std = 172), whereas total recording duration (without artifact rejection) was 1638 s (std = 168 s). For each window, we computed the logarithm of Hjorth activity, equal to windowed signal variance (Hjorth, 1970). The logarithm served to bring the data distribution closer to normal. For the source-reconstructed data, we averaged Hjorth activity across all grid points belonging to the same cortical parcel to obtain one feature per cortical area and time window.

$$\text{Hjorth activity}(x(t)) = \text{var}(x(t))$$

The use of Hjorth activity rather than spectral power or connectivity was motivated by the intention to compare decoding performance across brain areas while keeping the number of features as low as possible to avoid overfitting. Thus, we preferred metrics without frequency-resolution, uniquely associated with a single area. Our analysis choices were guided by the work of Yao et al. who performed a detailed investigation of the optimal choices for automated tremor detection (Yao et al., 2020). The authors tested several features and identified Hjorth activity as one of the most useful features. Further, they found XGBoost to be the best performing machine learning model among several candidates, and 1 s to be a good window size.

2.8. Machine learning

To predict the four different motor states from Hjorth activity, we performed 4-label classification on the windowed data using 5-fold, shuffled cross-validation. The XGBoost algorithm was used to perform the classification. XGBoost is an advanced decision-tree-based algorithm, widely used machine learning (Chen and Guestrin, 2016). It often provides better results than linear models and requires relatively small amounts of training data. Since the number of windows differed substantially between behavioral states both within and between subjects (Table 2), we used balanced accuracy, defined as the mean of sensitivity and specificity averaged across classes, as a measure of performance (Kelleher et al., 2020). When training the model, we used oversampling via *imbalanced-learn* toolbox (Lemaître et al., 2017) to artificially balance classes. The entire python & Matlab pipeline code (including preprocessing, source reconstruction and machine learning) is available at the code repository https://github.com/todorovdi/ContBehFeatExplorer.

2.9. LFP channel selection and hyperparameter tuning

For each subject, we performed single-feature classification for each LFP channel separately and selected the channel with best out-of-sample performance. Similarly, hyperparameter tuning was done by sampling combinations of the XGboost parameters *max_depth*, *min_child_weight*, *subsample* and *eta* and selecting the combination giving the best 5-fold cross-validated balanced accuracy. Neither LFP channel selection nor tuning had a strong effect on performance. All selected LFP channels were located contralateral to movement, except for patient S05.

3. Results

3.1. Distinguishing movements based on STN activity

We investigated how well the different motor states could be distinguished based on subthalamic activity alone. Fig. 2 shows a confusion matrix for each subject and medication state, providing discrimination performance for each pair of movements. STN activity alone turned out to be a rather weak predictor of movement type. In medication OFF (N = 6), the average percentage of correctly classified windows was 62% for quiet (std = 5%), 32% for rest tremor (std = 19%), 34% for hold (std = 16%), and 23% for grasp (std = 27%). The most common misclassification was labeling tremor as hold (mean number of cases = 22%, std = 9%). The least common misclassification was labeling tremor as grasp (mean = 8%, std = 8%). Random shuffling of labels lowered performance, demonstrating that the STN did provide relevant information (Table 3).

Levodopa did not have a strong influence on movement discrimination (Table 3). Balanced accuracy did not differ significantly between medication states (p = 0.7, all vs. all, independent t-test, N_{OFF} = 6, N_{ON} = 5).

In addition to the multiclass problem, we tested how well our approach can discriminate tremor from any other movement, as this classification is relevant for tremor therapy through adaptive DBS. When merging quiet, hold and grasp epochs into a single non-tremor class, we obtained balanced accuracy of 59% in the Med Off state (std = 8%) and 58% in Med On (std = 6%; Table 2). When discriminating merely between rest tremor and quiet, accuracy was 64% in Med Off (std = 4%) and 60% in Med On (std = 7%). This performance is similar to previous papers dealing with tremor vs. quiet (Hirschmann et al., 2017; Yao et al., 2020), taking into account that they reported regular, not balanced accuracy.

3.2. Distinguishing movements based on STN and cortical activity

When classifying epochs based on both subthalamic activity and the activity of all cortical parcels, we observed a strong increase in performance (average performance gain: 37%; Table 3 and Fig. 3). In medication OFF (N = 6), the average percentage of correctly classified epochs was 74% for quiet (std = 21%), 58% for rest tremor (std = 36%), 80% for hold (std = 12%), and 81% for grasp (std = 18%). The most common misclassification was labeling tremor as hold (mean = 22%, std = 31%). The least common misclassification was labeling rest tremor as grasp (mean = 1%, std = 1%). As in the STN-only case, random shuffling of labels lowered performance, lowering the number of classes increased performance, and medication had little influence on performance (p = 0.63, t-test; see Table 3).

When the model was trained across rather than within subjects, performance of all-to-all classification using STN LFP and MEG data dropped considerably, to 24% in medication OFF and to 28% in medication ON condition (compare Table 3), suggesting that movement-specific neural signatures vary across patients. When the model was trained on medication OFF data and tested on medication ON data of the same patient, mean balanced accuracy dropped to 31% (std = 12%). ON to OFF generalization was comparably poor (mean balanced accuracy = 23%, std = 4%), suggesting that movement-specific neural signatures vary across medication states as well.

3.3. STN-cortex two-feature models

While it would be difficult for an adaptive DBS system to monitor the entire cortex, it is feasible to monitor the STN and individual cortical areas (Gilron et al., 2021; Opri et al., 2020). Thus, we investigated the performance gain achieved by adding the activity of a single cortical area to STN activity as a second feature. Fig. 4 shows a brain map of the performance gain. In most cases, sensorimotor cortical areas added the most information.

Adding a single cortical area was usually enough to cover much of the total gain achievable by adding all cortical areas (Fig. 5). Adding all remaining cortical areas to the STN-cortex two-feature models as additional features led to an average performance increase of only 10% (std 11%) compared to the two-feature model.

The spatial distribution of information was not particularly lateralized. The single most informative cortical area was not always on the contralateral side with respect to movement, and adding all contralateral areas to STN activity did not consistently yield higher accuracy than adding all ipsilateral areas (Fig. 5). In this context, it is important to note that the non-moving hand was trembling in some of the patients and epochs. This likely contributes to the bilateral patterns.

4. Discussion

In this paper, we demonstrate the feasibility of distinguishing tremor from voluntary movements of the same hand. We found that LFP recordings from the STN are not sufficient for this distinction. It becomes possible, however, when considering additional cortical signals.

4.1. Previous studies

Distinguishing different movements in neural recordings has been the aim of several brain-computer interface studies, typically addressing cortical activity, as measured by EEG (Xu et al., 2021) or electrocorticography (ECoG) (Volkova et al., 2019). More recently, the possibility of recording subcortical activity in the context of

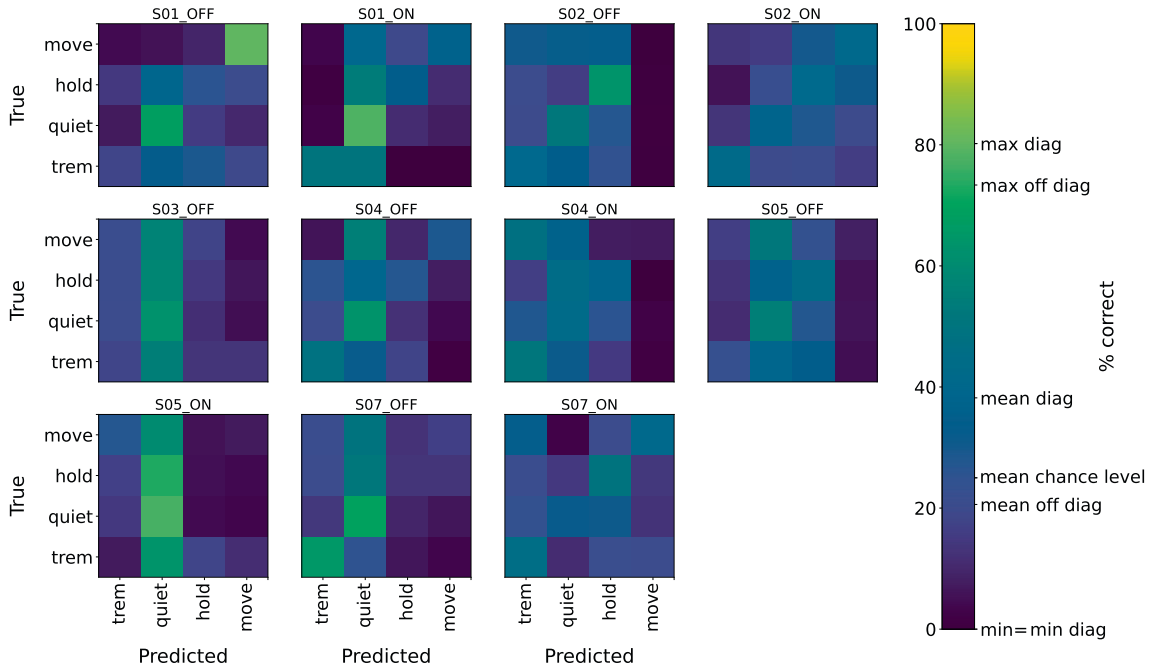

Fig. 2. Distinguishing movements based on subthalamic activity. Confusion matrices for Med Off and On per subject, averaged across cross-validation folds. The color bar shows the overall maximum and minimum, the maximum of all off-diagonal entries and the minimum of all diagonal entries, and the session-average chance level.

Table 3
Balanced accuracy, group results. "Shuffled" performance is 90% percentile of balanced accuracies obtained from 100 permutations of class labels. STN = subthalamic nucleus; LFP = local field potential.

Med	Data: STN LFP alone		**mean, %**	**std, %**	**Med**	Data: STN LFP + MEG		**mean, %**	**std, %**
	classification	**shuffling**				**classification**	**shuffling**		
OFF	all vs. all	no	38	8	OFF	all vs. all	no	73	22
OFF	all vs. all	yes	26	1	OFF	all vs. all	yes	25	1
OFF	trem vs. all other	no	59	8	OFF	trem vs. all other	no	78	19
OFF	trem vs. all other	yes	50	0	OFF	trem vs. all other	yes	50	0
OFF	trem vs. quiet	no	64	4	OFF	trem vs. quiet	no	80	16
OFF	trem vs. quiet	yes	51	1	OFF	trem vs. quiet	yes	50	0
ON	all vs. all	no	40	8	ON	all vs. all	no	79	9
ON	all vs. all	yes	26	0	ON	all vs. all	yes	25	1
ON	trem vs. all other	no	59	6	ON	trem vs. all other	no	86	8
ON	trem vs. all other	yes	50	0	ON	trem vs. all other	yes	50	0
ON	trem vs. quiet	no	60	8	ON	trem vs. quiet	no	87	8
ON	trem vs. quiet	yes	51	1	ON	trem vs. quiet	yes	51	1

DBS has facilitated classification studies in basal ganglia and thalamus, most of which deal with movement detection, i.e. the distinction between movement and rest. Loukas and Brown were the first to decode the onset of voluntary movements from subthalamic activity (Loukas and Brown, 2004). Several other studies aimed for tremor detection, due to its relevance for adaptive DBS (Bakstein et al., 2012; Camara et al., 2015; Hirschmann et al., 2017; Shah et al., 2018; Yao et al., 2020). Our group has previously applied Hidden Markov Modelling to STN LFPs, using a superset of the data analyzed here (Hirschmann et al., 2017). Spontaneously occurring PD rest tremor was detected with an average sensitivity of 70% and a specificity of 89%. Yao et al. achieved a sensitivity of 89% and a specificity of 50%, using XGBoost and Kalman filtering of selected input features (Yao et al., 2020). The same group later demonstrated the feasibility of XGBoost tremor detection on chip, facilitating its integration into small, battery-powered neurostimulators (Zhu et al., 2020).Tremor detection has also been demonstrated for thalamic LFPs recorded in ET patients (Tan et al., 2019), including the feasibility of conditioning DBS on these signals under laboratory conditions (He et al., 2021).

In this study, we obtained comparable tremor detection performance for the multi-feature case (STN + cortex). Importantly, this work goes a step further by distinguishing between tremor, tremor-free rest, self-paced fist-clenching and static forearm extension.

4.2. Clinical implications

Distinguishing between tremor and voluntary hand movements of the same limb based on brain activity is a challenging task, which has both clinical and basic science implications. From a clinical perspective, mastering this task would allow for better adaptation of DBS to the current situation, as it would reduce unnecessary stimulation occurring when an adaptive DBS system confuses voluntary movement, or dyskinesia, with tremor. Unnecessary stimulation is not only a waste of energy, but might contribute to maladaptive changes in response to DBS (Reich et al., 2016). In addition, an unnecessary sudden onset of stimulation or a sudden amplitude increase may interfere with fine motor control, as both may elicit transient side-effects such as paresthesia.

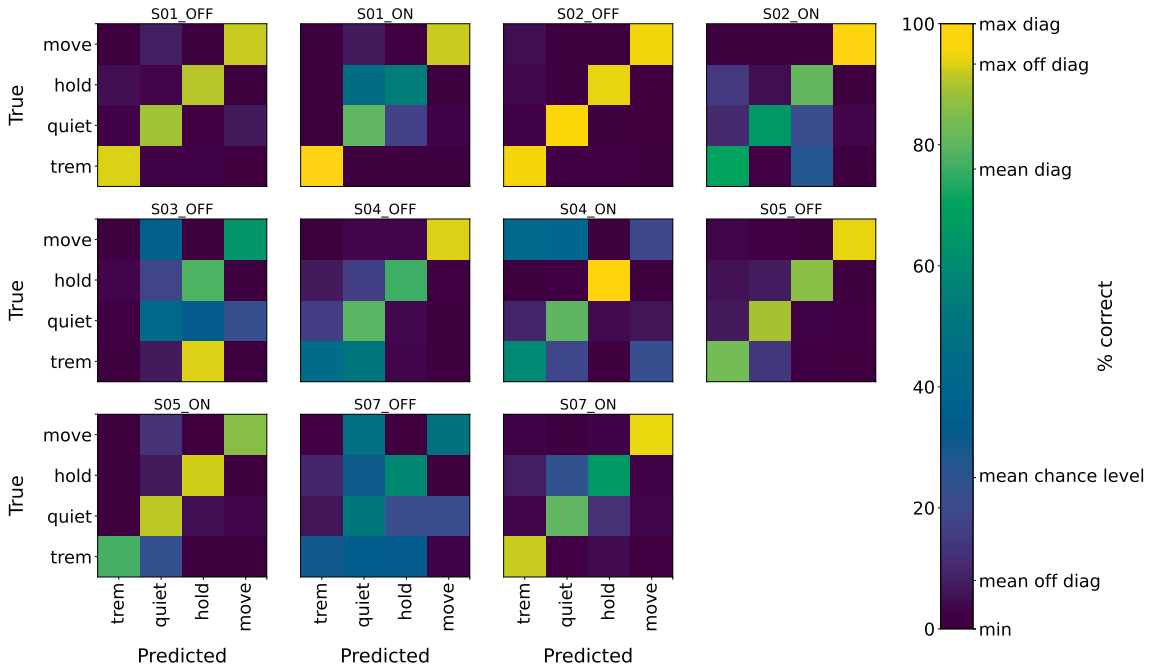

Fig. 3. Distinguishing movements based on subthalamic and cortical activity. Confusion matrices for Med On and Med Off per subject, averaged across cross-validation folds. The color bar shows the overall maximum, the maximum of all off-diagonal entries and the minimum of all diagonal entries, and the session-average chance level.

4.3. Neuroscientific implications

From a basic science perspective, it is warranted to understand the neurophysiological differences between voluntary and non-voluntary movements such as tremor. Tremor and voluntary movement share a common oscillatory signature, characterized by beta desynchronization and gamma synchronization (Beudel et al., 2015; Pfurtscheller et al., 2003; Qasim et al., 2016; Wang et al., 2005). While this pattern is very robust, it signals the presence of any movement rather than what movement is being executed, nor whether the movement is voluntary or not. The latter question is highly interesting for general neuroscience and has been addressed by contrasting tremor and mimicked tremor. Although some differences emerged, there were generally more similarities than differences (Muthuraman et al., 2018, 2012). Hence, there is currently no consensus on the neural mechanisms underlying involuntary movement and hence no compelling explanation of why tremor cannot be stopped at will.

Even without a neural correlate of volition, it may be possible to distinguish tremor from other movements based on brain signals. A smart DBS system could simply try to detect oscillatory movements of a certain frequency and assume tremor, as rhythmic movements of this kind are rarely voluntary. This appears to be a feasible approach, given the presumably unique neural correlates of such movements, such as an increase of power at individual tremor frequency (Hirschmann et al., 2013a; Pollok et al., 2004; Timmermann et al., 2003). The characteristic kinematics of tremor and its reflection in brain activity is most likely the reason why were able to distinguish it from other movements here. Note, however, that our approach was based on Hjorth activity, which is not frequency-resolved. Thus, knowing the individual tremor frequency is not necessary for tremor discrimination.

4.4. Movement-related information in STN and cortex

One of the key findings of this paper is that cortical signals can dramatically increase tremor discrimination. This observation tallies with recent studies in PD patients decoding grip force from STN and primary motor cortex, the latter recorded through intraoperative ECoG (Merk et al., 2022; Peterson et al., 2023). Both studies achieved much better predictions when using cortical signals, as compared to subthalamic signals. The authors restrained from drawing conclusions about the information content of cortex versus STN because ECoG signals have a better signal-to-noise ration than recordings made with a DBS electrode, which might explain the difference in performance. In our case, however, the invasive deep brain recording is generally considered to have better signal-to-noise ratio than the noninvasive MEG, suggesting that the STN might not be the optimal brain area for inferring the kind of movement being performed. In fact, a number of studies indicate that the basal ganglia control movement vigor, i.e. the strength and velocity of a movement, rather than being concerned with movement coordination (Dudman and Krakauer, 2016; Lofredi et al., 2018; Turner and Desmurget, 2010; Yttri and Dudman, 2016). This may imply that STN activity is more useful for predicting grip force (Merk et al., 2022; Shah et al., 2018) than movement type.

While the observations discussed above are in line with the poor decoding of movement type based on STN activity alone, as observed here and in a different analysis of the same data (Hirschmann et al., 2017), it is challenged by recent findings of Golshan and colleagues, who managed to decode different voluntary movements from STN LFPs with accuracies of up to 90% (Golshan et al., 2020, 2018). These studies did not investigate tremor, however, and the approach requires knowing when a movement is initiated. This information, of course, would not be available when applying adaptive DBS in practice.

So as of now, it seems that any smart DBS system that needs know to more about a patient's motor state than whether or not the patient is at rest would likely profit substantially from external information, such as peripherals (Cagnan et al., 2017; Cernera et al., 2021; Malekmohammadi et al., 2016) or electrodes in additional brain areas. If so, how many and which brain areas should be monitored? Our results suggest that a few areas suffice for distinguishing tremor from voluntary movement and between different voluntary movements. Unsurprisingly, primary and premotor areas were found to be most useful, although other areas con-

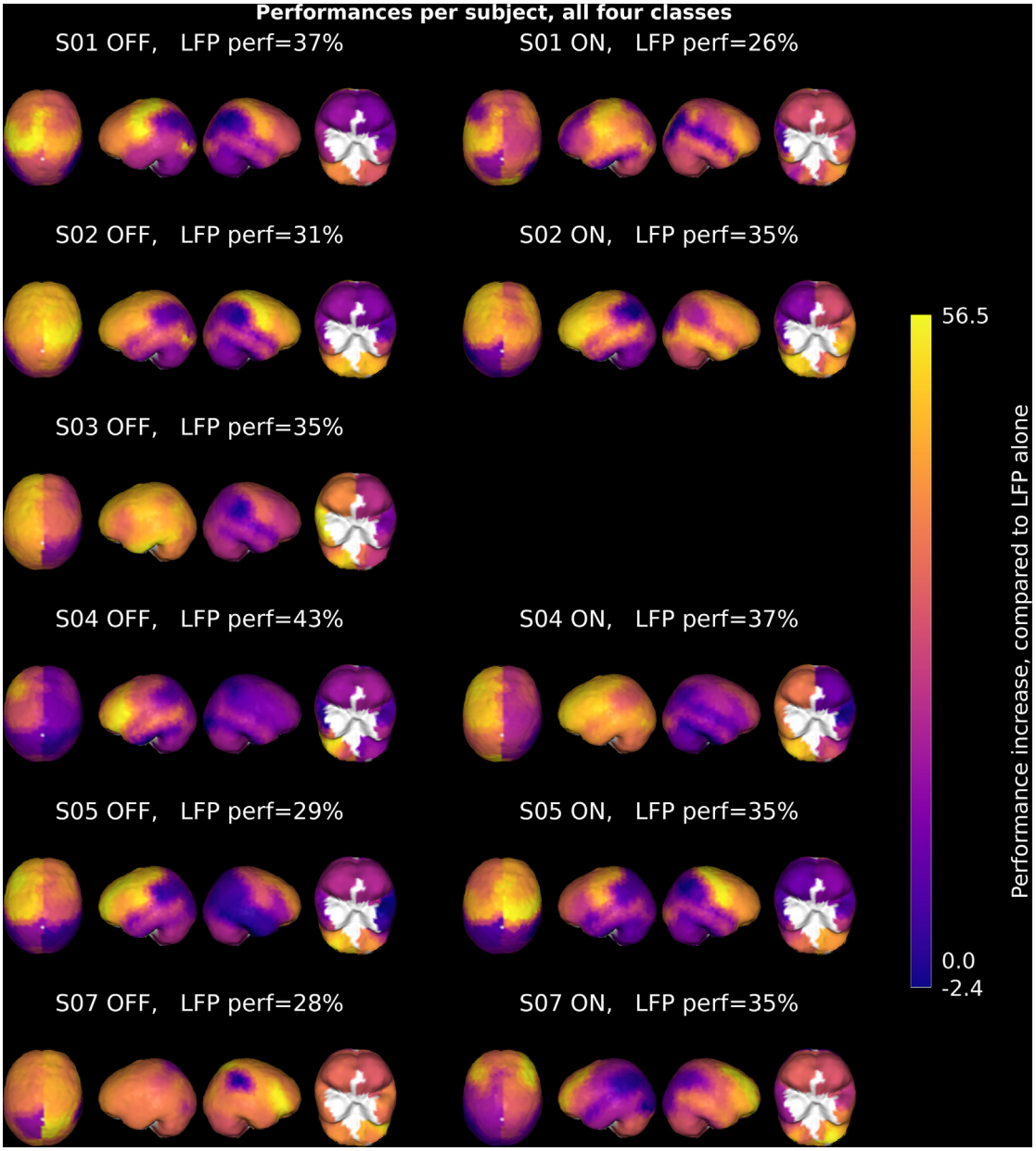

Fig. 4. Gain of using cortical activity in addition subthalamic nucleus activity. The balanced accuracy achieved with subthalamic activity alone is provided in the headings ("LFP perf"). Colors code the improvement (in %) obtained by adding the activity of an individual cortical brain area as a second feature. LFP = local field potential.

tributed information as well. Thus, a system monitoring both STN and motor cortex appears promising for real-time motor state discrimination in PD.

In fact, such systems have already been tested both in-clinic and at home. Using an implantable DBS system capable of recording neural activity and a combination of deep brain electrodes and cortical strip electrodes placed on primary motor cortex, Gilron et al. found that conditioning STN DBS on cortical gamma oscillations increased the time spent in the Med On/Stim On state without experiencing dyskinesia (Gilron et al., 2021). This is a crucial finding, since reducing stimulation-induced side effects is a key promise of adaptive DBS. Using a similar approach, Opri et al. demonstrated that conditioning thalamic DBS on motorcortical low-frequency activity is as effective for suppressing essential tremor as standard DBS, despite delivering less energy (Opri et al., 2020).

4.5. Generalizability of movement decoding

To be useful in practice, a decoding approach needs to work equally well in different situations, e.g. before and after intake of anti-Parkinsonian medication. In agreement with (Golshan et al., 2020), we obtained similar decoding performance in medication On and Off. This needs to be tested further, however, in light of recent findings linking decoding performance to motor impairment (Merk et al., 2022; Peterson et al., 2023), which is closely linked to dopamine availability. Although it was possible to achieve decent decoding in both medication states, each state required a different decoder. While this is clearly suboptimal for clinical application, it may turn out to be a minor hurdle, as PD patients rarely reach a complete OFF state when medicated properly. In practice, an ON-state decoder might suffice for most patients.

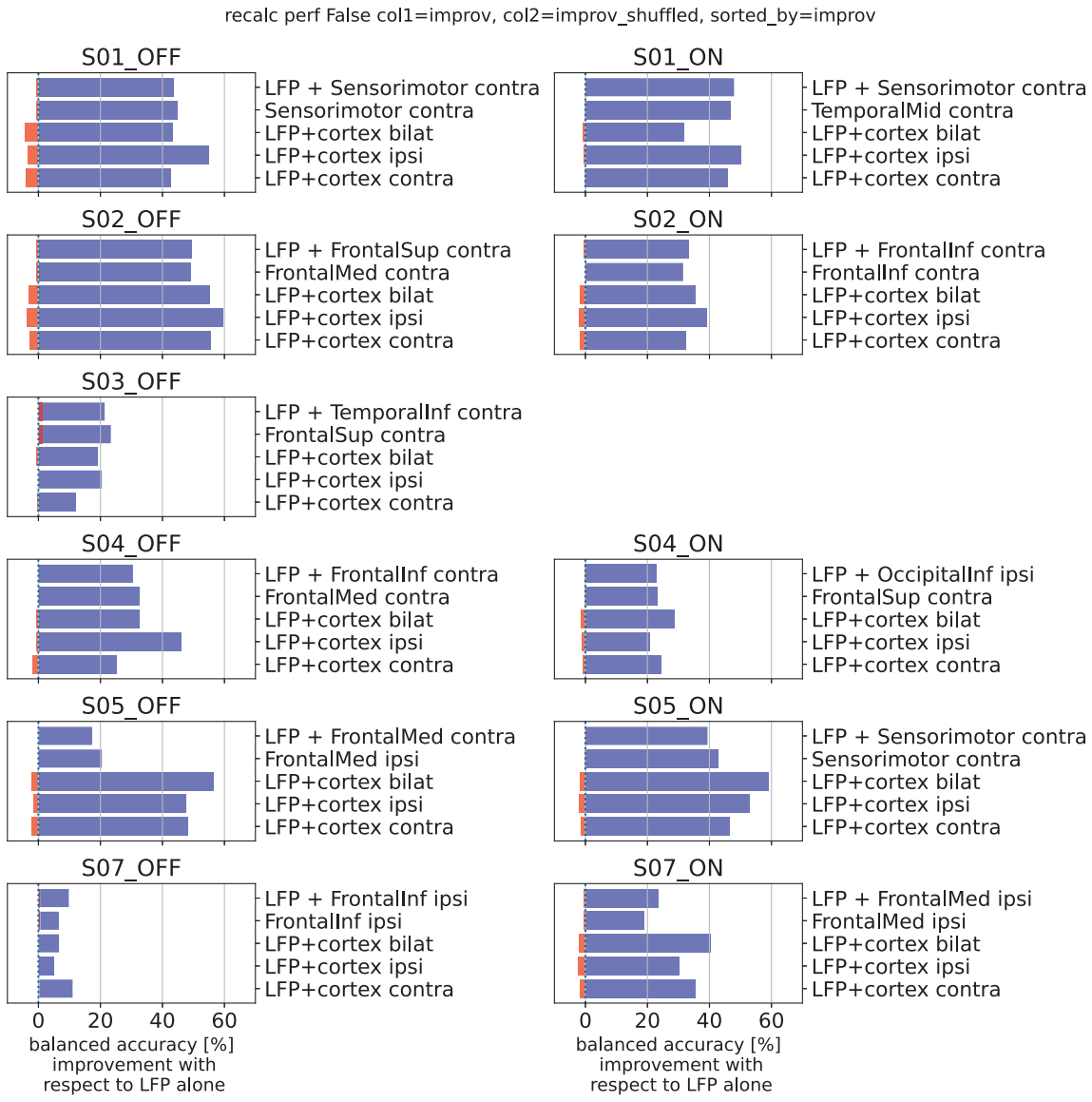

Fig. 5. Most informative cortical areas and lateralization of information. Bar height indicates the performance difference with respect to the STN-only case, with original (blue) and shuffled class labels (red). Uppermost bar: best combination of one STN feature and one cortical feature. Second bar: best single cortical feature (STN not used). The lower three bars illustrate the gain of adding all cortical areas (both hemispheres), only the ipsilateral areas (with respect to the moving hand) and only the contralateral areas, respectively. LFP = local field potential; STN = subthalamic nucleus.

Ideally, a decoder would not only generalize to different dopamine levels but also to different patients. As in almost all previous works on this topic (but see Hirschmann et al., 2022), our approach required within-patient training, i.e. a decoder working in one patient does not necessarily work in another. Tuning the decoder to a new patient requires individual, electrophysiological data from the DBS target and cortex. While this seemed infeasible a few years ago, the advent of new DBS systems capable of recording brain signals in addition to delivering stimulation has made this scenario more realistic (Jimenez-Shahed, 2021). Note, however, that a general decoder would still be preferable from both a practical point of view (no tuning necessary) and a basic science perspective because only general decoders allow for conclusions on the general mechanism of tremor.

4.6. Limitations

One obvious limitation of this work is that we did not detect tremor in real-time nor condition DBS on tremor. In addition, the performance achieved here is not enough for clinical application, although much better than chance, as evidenced by the decline caused by shuffling class labels randomly. Moreover, due to a limited amount of data, parts of the training data were close in time to parts of the test data, which might cause overfitting in the presence of temporal autocorrelation. In this scenario, the classifier groups epochs based on their closeness in time rather than their movement class. This potential confound can be mitigated in larger datasets by requiring e.g. a certain distance in time between all train and test epochs.

Further, the cortical signal was recorded with MEG rather than ECoG. While MEG has much worse spatial resolution, it offers whole-brain coverage. This allows us to exclude movement artifacts as the true source of information because artifacts have a different topography than the information maps provided here (Kandemir et al., 2020). While we found most information in sensorimotor regions, DBS hardware-related artifacts are centered on the adapter for the externalized lead (right parietal and right temporal regions) whereas movement-related MEG artifacts are strongest close to the moving limb.

Finally, we included only men in this re-analysis because they happened to fulfill the inclusion criteria accidentally (spontaneous

waxing and waning of tremor in the limb used in the motor task and presence of both hold and grasp movements in the recordings). Hence, we cannot be sure that our findings are transferable to females. Yet, we see no reason for assuming sex differences.

4.7. Conclusions

PD rest tremor can be distinguished from voluntary hand movements when considering subthalamic and cortical signals. This distinction is possible regardless of the dopamine level.

Funding

This work was supported by Brunhilde Moll Stiftung. Dmitrii Todorov was supported by European Commissions' MSCA-IF-2017 Grant 793834.

Conflict of interest

None of the authors have potential conflicts of interest to be disclosed.

CRediT authorship contribution statement

Dmitrii Todorov: Conceptualization, Writing – review & editing, Visualization, Writing – original draft, Project administration, Investigation, Software, Methodology, Formal analysis, Funding acquisition. **Alfons Schnitzler:** Funding acquisition, Resources, Writing – review & editing. **Jan Hirschmann:** Writing – original draft, Methodology, Supervision, Validation, Project administration, Data curation, Writing – review & editing, Conceptualization.

Acknowledgement

Dmitrii Todorov acknowledges helpful advice about data management and processing from Alexandra Steina and Marius Kroesche. Computations were largely made possible thanks to Human Brain Project ICEI computing resources (project icei-hpb-2020–0012).

References

Bakstein E, Burgess J, Warwick K, Ruiz V, Aziz T, Stein J. Parkinsonian tremor identification with multiple local field potential feature classification. J Neurosci Methods 2012;209:320–30. https://doi.org/10.1016/j.jneumeth.2012.06.027.

Beudel M, Little S, Pogosyan A, Ashkan K, Foltynie T, Limousin P, et al. Tremor reduction by deep brain stimulation is associated with gamma power suppression in Parkinson's disease. Neuromodulation Technol Neural Interface 2015;18:349–54.

Cagnan H, Pedrosa D, Little S, Pogosyan A, Cheeran B, Aziz T, et al. Stimulating at the right time: phase-specific deep brain stimulation. Brain 2017;140:132–45. https://doi.org/10.1093/brain/aww286.

Camara C, Isasi P, Warwick K, Ruiz V, Aziz T, Stein J, et al. Resting tremor classification and detection in Parkinson's disease patients. Biomed Signal Process Control 2015;16:88–97. https://doi.org/10.1016/j.bspc.2014.09.006.

Cernera S, Alcantara JD, Opri E, Cagle JN, Eisinger RS, Boogaart Z, et al. Wearable sensor-driven responsive deep brain stimulation for essential tremor. Brain Stimul 2021;14:1434–43. https://doi.org/10.1016/j.brs.2021.09.002.

Chen T, Guestrin C. XGBoost: A Scalable Tree Boosting System. In: Proc. 22nd ACM SIGKDD Int. Conf. Knowl. Discov. Data Min., New York, NY, USA: Association for Computing Machinery; 2016, p. 785–94. https://doi.org/10.1145/2939672.2939785.

Dale J, Schmidt SL, Mitchell K, Turner DA, Grill WM. Evoked potentials generated by deep brain stimulation for Parkinson's disease. Brain Stimul 2022;15:1040–7. https://doi.org/10.1016/j.brs.2022.07.048.

Dudman JT, Krakauer JW. The basal ganglia: from motor commands to the control of vigor. Curr Opin Neurobiol 2016;37:158–66. https://doi.org/10.1016/j.conb.2016.02.005.

Gilron R, Little S, Perrone R, Wilt R, de Hemptinne C, Yaroshinsky MS, et al. Long-term wireless streaming of neural recordings for circuit discovery and adaptive stimulation in individuals with Parkinson's disease. Nat Biotechnol 2021;39:1078–85. https://doi.org/10.1038/s41587-021-00897-5.

Golshan HM, Hebb AO, Hanrahan SJ, Nedrud J, Mahoor MH. A hierarchical structure for human behavior classification using STN local field potentials. J Neurosci Methods 2018;293:254–63. https://doi.org/10.1016/j.jneumeth.2017.10.001.

Golshan HM, Hebb AO, Mahoor MH. LFP-Net: a deep learning framework to recognize human behavioral activities using brain STN-LFP signals. J Neurosci Methods 2020;335. https://doi.org/10.1016/j.jneumeth.2020.108621 108621.

Gramfort A, Luessi M, Larson E, Engemann DA, Strohmeier D, Brodbeck C, et al. MNE software for processing MEG and EEG data. NeuroImage 2014;86:446–60. https://doi.org/10.1016/j.neuroimage.2013.10.027.

He S, Baig F, Mostofi A, Pogosyan A, Debarros J, Green AL, et al. Closed-Loop deep brain stimulation for essential tremor based on thalamic local field potentials. Mov Disord 2021:mds.28513. https://doi.org/10.1002/mds.28513.

Helmich RC. The cerebral basis of Parkinsonian tremor: a network perspective. Mov Disord 2018;33:219–31.

Hirschmann J, Butz M, Hartmann CJ, Hoogenboom N, Özkurt TE, Vesper J, et al. Parkinsonian rest tremor is associated with modulations of subthalamic high-frequency oscillations. Mov Disord 2016;31:1551–9. https://doi.org/10.1002/mds.26663.

Hirschmann J, Hartmann CJ, Butz M, Hoogenboom N, Özkurt TE, Elben S, et al. A direct relationship between oscillatory subthalamic nucleus–cortex coupling and rest tremor in Parkinson's disease. Brain 2013a;136:3659–70. https://doi.org/10.1093/brain/awt271.

Hirschmann J, Özkurt TE, Butz M, Homburger M, Elben S, Hartmann C, et al. Differential modulation of STN-cortical and cortico-muscular coherence by movement and levodopa in Parkinson's disease. Neuroimage 2013b;68:203–13.

Hirschmann J, Schoffelen J, Schnitzler A, Van Gerven M. Parkinsonian rest tremor can be detected accurately based on neuronal oscillations recorded from the subthalamic nucleus. Clin Neurophysiol 2017;128:2029–36.

Hirschmann J, Steina A, Vesper J, Florin E, Schnitzler A. Neuronal oscillations predict deep brain stimulation outcome in Parkinson's disease. Brain Stimul 2022;15:792–802. https://doi.org/10.1016/j.brs.2022.05.008.

Hjorth B. EEG analysis based on time domain properties. Electroencephalogr Clin Neurophysiol 1970;29:306–10. https://doi.org/10.1016/0013-4694(70)90143-4.

Horn A, Kühn AA. Lead-DBS: A toolbox for deep brain stimulation electrode localizations and visualizations. NeuroImage 2015;107:127–35. https://doi.org/10.1016/j.neuroimage.2014.12.002.

Jimenez-Shahed J. Device profile of the percept PC deep brain stimulation system for the treatment of Parkinson's disease and related disorders. Expert Rev Med Devices 2021;18:319–32. https://doi.org/10.1080/17434440.2021.1909471.

Kandemir AL, Litvak V, Florin E. The comparative performance of DBS artefact rejection methods for MEG recordings. NeuroImage 2020;219. https://doi.org/10.1016/j.neuroimage.2020.117057 117057.

Kelleher JD, Namee BM, D'Arcy A. Fundamentals of Machine Learning for Predictive Data Analytics, second edition: Algorithms, Worked Examples, and Case Studies. MIT Press; 2020.

Koeglsperger T, Palleis C, Hell F, Mehrkens JH, Bötzel K. Deep brain stimulation programming for movement disorders: current concepts and evidence-based strategies. Front Neurol 2019;10. https://doi.org/10.3389/fneur.2019.00410.

Krauss JK, Lipsman N, Aziz T, Boutet A, Brown P, Chang JW, et al. Technology of deep brain stimulation: current status and future directions. Nat Rev Neurol 2021;17:75–87. https://doi.org/10.1038/s41582-020-00426-z.

Lemaître G, Nogueira F, Aridas CK. Imbalanced-learn: a python toolbox to tackle the curse of imbalanced datasets in machine learning. J Mach Learn Res 2017;18:559–63.

Little S, Beudel M, Zrinzo L, Foltynie T, Limousin P, Hariz M, et al. Bilateral adaptive deep brain stimulation is effective in Parkinson's disease. J Neurol Neurosurg Psychiatry 2016;87:717–21. https://doi.org/10.1136/jnnp-2015-310972.

Little S, Pogosyan A, Neal S, Zavala B, Zrinzo L, Hariz M, et al. Adaptive deep brain stimulation in advanced Parkinson disease. Ann Neurol 2013;74:449–57. 10/gcb5dd.

Lofredi R, Neumann W-J, Bock A, Horn A, Huebl J, Siegert S, et al. Dopamine-dependent scaling of subthalamic gamma bursts with movement velocity in patients with Parkinson's disease. ELife 2018;7:e31895.

Loukas C, Brown P. Online prediction of self-paced hand-movements from subthalamic activity using neural networks in Parkinson's disease. J Neurosci Methods 2004;137:193–205. https://doi.org/10.1016/j.jneumeth.2004.02.017.

Malekmohammadi M, Herron J, Velisar A, Blumenfeld Z, Trager MH, Chizeck HJ, et al. Kinematic adaptive deep brain stimulation for resting tremor in Parkinson's disease. Mov Disord 2016;31:426–8. https://doi.org/10.1002/mds.26482.

Marceglia S, Guidetti M, Harmsen IE, Loh A, Meoni S, Foffani G, et al. Deep brain stimulation: is it time to change gears by closing the loop? J Neural Eng 2021;18. https://doi.org/10.1088/1741-2552/ac3267 061001.

Meidahl AC, Tinkhauser G, Herz DM, Cagnan H, Debarros J, Brown P. Adaptive deep brain stimulation for movement disorders: the long road to clinical therapy: adaptive DBS review. Mov Disord 2017;32:810–9. https://doi.org/10.1002/mds.27022.

Merk T, Peterson V, Lipski WJ, Blankertz B, Turner RS, Li N, et al. Electrocorticography is superior to subthalamic local field potentials for movement decoding in Parkinson's disease. ELife 2022;11:e75126.

Milosevic L, Kalia SK, Hodaie M, Lozano AM, Popovic MR, Hutchison WD. Physiological mechanisms of thalamic ventral intermediate nucleus stimulation for tremor suppression. Brain 2018;141:2142–55. 10/gdwzfx.

Muthuraman M, Heute U, Arning K, Anwar AR, Elble R, Deuschl G, et al. Oscillating central motor networks in pathological tremors and voluntary movements.

What makes the difference? NeuroImage 2012;60:1331–9. https://doi.org/10.1016/j.neuroimage.2012.01.088.
Muthuraman M, Raethjen J, Koirala N, Anwar AR, Mideksa KG, Elble R, et al. Cerebello-cortical network fingerprints differ between essential, Parkinson's and mimicked tremors. Brain 2018;141:1770–81. https://doi.org/10.1093/brain/awy098.
Neumann W-J, Turner RS, Blankertz B, Mitchell T, Kühn AA, Richardson RM. Toward electrophysiology-based intelligent adaptive deep brain stimulation for movement disorders. Neurotherapeutics 2019;16:105–18. https://doi.org/10.1007/s13311-018-00705-0.
Nolte G. The magnetic lead field theorem in the quasi-static approximation and its use for magnetoencephalography forward calculation in realistic volume conductors. Phys Med Biol 2003;48:3637. https://doi.org/10.1088/0031-9155/48/22/002.
Oostenveld R, Fries P, Maris E, Schoffelen J-M. FieldTrip: open source software for advanced analysis of MEG, EEG, and invasive electrophysiological data. Comput Intell Neurosci 2011;1(1–1):9. https://doi.org/10.1155/2011/156869.
Opri E, Cernera S, Molina R, Eisinger RS, Cagle JN, Almeida L, et al. Chronic embedded cortico-thalamic closed-loop deep brain stimulation for the treatment of essential tremor. Sci Transl Med 2020;12. https://doi.org/10.1126/scitranslmed.aay7680 eaay7680.
Peterson V, Merk T, Bush A, Nikulin V, Kühn AA, Neumann W-J, et al. Movement decoding using spatio-spectral features of cortical and subcortical local field potentials. Exp Neurol 2023;359. https://doi.org/10.1016/j.expneurol.2022.114261 114261.
Pfurtscheller G, Graimann B, Huggins JE, Levine SP, Schuh LA. Spatiotemporal patterns of beta desynchronization and gamma synchronization in corticographic data during self-paced movement. Clin Neurophysiol 2003;114:1226–36. https://doi.org/10.1016/S1388-2457(03)00067-1.
Piña-Fuentes D, Little S, Oterdoom M, Neal S, Pogosyan A, Tijssen MAJ, et al. Adaptive DBS in a Parkinson's patient with chronically implanted DBS: a proof of principle. Mov Disord 2017;32:1253–4. https://doi.org/10.1002/mds.26959.
Pollok B, Gross J, Dirks M, Timmermann L, Schnitzler A. The cerebral oscillatory network of voluntary tremor. J Physiol 2004;554:871–8. https://doi.org/10.1113/jphysiol.2003.051235.
Qasim SE, de Hemptinne C, Swann NC, Miocinovic S, Ostrem JL, Starr PA. Electrocorticography reveals beta desynchronization in the basal ganglia-cortical loop during rest tremor in Parkinson's disease. Neurobiol Dis 2016;86:177–86.
Reich MM, Brumberg J, Pozzi NG, Marotta G, Roothans J, Åström M, et al. Progressive gait ataxia following deep brain stimulation for essential tremor: adverse effect or lack of efficacy? Brain 2016;139:2948–56. https://doi.org/10.1093/brain/aww223.
Shah SA, Tinkhauser G, Chen CC, Little S, Brown P. Parkinsonian Tremor Detection from Subthalamic Nucleus Local Field Potentials for Closed-Loop Deep Brain Stimulation. In: 2018 40th Annu. Int. Conf. IEEE Eng. Med. Biol. Soc. EMBC, Honolulu, HI: IEEE; 2018, p. 2320–4. https://doi.org/10.1109/EMBC.2018.8512741.
Swann NC, de Hemptinne C, Thompson MC, Miocinovic S, Miller AM, Gilron R, et al. Adaptive deep brain stimulation for Parkinson's disease using motor cortex sensing. J Neural Eng 2018;15. https://doi.org/10.1088/1741-2552/aabc9b 046006.
Tan H, Debarros J, He S, Pogosyan A, Aziz TZ, Huang Y, et al. Decoding voluntary movements and postural tremor based on thalamic LFPs as a basis for closed-loop stimulation for essential tremor. Brain Stimul 2019;12:858–67. https://doi.org/10.1016/j.brs.2019.02.011.
Taulu S, Simola J. Spatiotemporal signal space separation method for rejecting nearby interference in MEG measurements. Phys Med Biol 2006;51:1759–68. https://doi.org/10.1088/0031-9155/51/7/008.
Timmermann L, Gross J, Dirks M, Volkmann J, Freund H-J, Schnitzler A. The cerebral oscillatory network of parkinsonian resting tremor. Brain 2003;126:199–212. https://doi.org/10.1093/brain/awg022.
Tinkhauser G, Pogosyan A, Little S, Beudel M, Herz DM, Tan H, et al. The modulatory effect of adaptive deep brain stimulation on beta bursts in Parkinson's disease. Brain 2017;140:1053–67.
Turner RS, Desmurget M. Basal ganglia contributions to motor control: a vigorous tutor. Curr Opin Neurobiol 2010;20:704–16. https://doi.org/10.1016/j.conb.2010.08.022.
Tzourio-Mazoyer N, Landeau B, Papathanassiou D, Crivello F, Etard O, Delcroix N, et al. Automated anatomical labeling of activations in SPM using a macroscopic anatomical parcellation of the MNI MRI single-subject brain. NeuroImage 2002;15:273–89. https://doi.org/10.1006/nimg.2001.0978.
Volkova K, Lebedev MA, Kaplan A, Ossadtchi A. Decoding movement from electrocorticographic activity: a review. Front Neuroinformatics 2019;13. https://doi.org/10.3389/fninf.2019.00074.
Wang S-Y, Aziz TZ, Stein JF, Liu X. Time–frequency analysis of transient neuromuscular events: dynamic changes in activity of the subthalamic nucleus and forearm muscles related to the intermittent resting tremor. J Neurosci Methods 2005;145:151–8. https://doi.org/10.1016/j.jneumeth.2004.12.009.
Xu L, Xu M, Jung T-P, Ming D. Review of brain encoding and decoding mechanisms for EEG-based brain–computer interface. Cogn Neurodyn 2021;15:569–84. https://doi.org/10.1007/s11571-021-09676-z.
Yao L, Brown P, Shoaran M. Improved detection of Parkinsonian resting tremor with feature engineering and Kalman filtering. Clin Neurophysiol 2020;131:274–84. https://doi.org/10.1016/j.clinph.2019.09.021.
Yttri EA, Dudman JT. Opponent and bidirectional control of movement velocity in the basal ganglia. Nature 2016;533:402–6. https://doi.org/10.1038/nature17639.
Zarzycki MZ, Domitrz I. Stimulation-induced side effects after deep brain stimulation – a systematic review. Acta Neuropsychiatr 2020;32:57–64. 10/gpn2xw.
Zhu B, Farivar M, Shoaran M. ResOT: resource-efficient oblique trees for neural signal classification. IEEE Trans Biomed Circuits Syst 2020;14:692–704. https://doi.org/10.1109/TBCAS.2020.3004544.